

DeepFloat: Resource-Efficient Dynamic Management of Vehicular Floating Content

Geatano Manzo^{1,2}, Sebastian Otálora¹, Marco Ajmone Marsan³, Torsten Braun², Hung Nguyen⁴, Gianluca Rizzo¹

¹University of Applied Science Western Switzerland – {name.surname}@hevs.ch

²University of Bern, Switzerland – braun@inf.unibe.ch

³IMDEA Networks Institute, Spain & Politecnico di Torino, Italy – ajmone@polito.it

⁴University of Adelaide, Australia – hung.nguyen@adelaide.edu.au

Abstract—Opportunistic communications are expected to play a crucial role in vehicular services that are based on location and require extremely low latency. A widely investigated opportunistic communication paradigm for the local dissemination of contextualized information is Floating Content (FC), which tries to make content float over a geographical area by replicating it whenever two users meet. The key Quality of Service (QoS) indicator for FC is *content availability*, defined as the fraction of users that received the information that is supposed to float.

Optimizing the use of FC resources while meeting the availability target QoS is a highly complex issue. Fully distributed, distance-based approaches proved to be highly inefficient, and may not meet the target QoS. Centralized, model-based approaches do not perform well in realistic inhomogeneous settings.

In this work, we present a data-driven centralized approach to resource-efficient, QoS-aware dynamic management of FC. We propose a Deep Learning strategy for FC operation, which employs a Convolutional Neural Network (CNN) to capture the relations between the patterns of users mobility, the patterns of content diffusion and replication, and the performance of FC in terms of resource efficiency and availability within a given Zone of Interest (ZOI).

Numerical evaluations show the effectiveness of our approach, as well as the capability of our approach to adapt to mobility pattern changes over time.

I. INTRODUCTION

Vehicular communications are considered one of the key vertical application domains for 5G [1], and a version of the IEEE 802.11 standards is specifically devoted to vehicular environments [2]. The two standards serve different purposes. Indeed, while some vehicular services are better served through a cellular infrastructure, others are more naturally mapped onto opportunistic communication schemes, especially those that are based on vehicle location and require extremely low latency.

Several opportunistic communication paradigms for the local dissemination of contextualized information have been proposed. Relevant examples are Floating Content, or Hovering Information (see [3]–[6] and literature therein). They all aim at the local dissemination of information to end users over a defined geographic area (called Anchor Zone or AZ) through direct terminal-to-terminal connectivity. In what follows, we will refer to this approach as *FC*, though our results apply to the whole family of techniques. FC aims to minimize the

usage of resources (such as bandwidth and memory) within the AZ, while achieving a given performance target. Typically, FC performance at a given time instant is defined in terms of *success ratio*, i.e., the average fraction of nodes with content at a given location (henceforth denoted as *Zone of Interest* or ZOI). FC paradigms find applications in several scenarios such as urban environments [7] and university campus contexts [8], for location-aware services.

Performance studies of FC schemes can be categorized into two broad classes. On one side, many works focus on content persistence over time and propose heuristics for guaranteeing content persistence within a predefined region, which usually coincides with the AZ itself [3]. Such heuristics are often tailored to a specific context (such as highways, or pedestrians in city squares [9]) and quite surprisingly, assume that a high likelihood of content persistence is sufficient to successfully support such applications as notifications of car accidents or traffic congestion. Hence they are hard to generalize and to be used to support applications that need a minimum amount of delivered contents within a given area.

Another class of proposals adopts a model-based approach to FC dimensioning, usually based on the mean field approximation of the dynamics of the population of users with content, and on the assumptions of stationarity of the mobility patterns and uniformity of user distribution in space [3]–[9]. In these formulations, the FC dimensioning problem boils down to finding the minimum radius of a circular AZ area, which guarantees a given minimum content lifetime, and/or a target success ratio. However, models based on mean field approximation require a large enough population of users to yield accurate results, and this imposes a coarse granularity in the way in which resources are partitioned and managed. This leads to suboptimal AZ configurations, often including users who do not contribute significantly to FC performance, and hence large resource inefficiencies. Moreover, such approaches do not lend themselves to generalizations to more realistic settings characterized by heterogeneous user distributions (and in particular to user clustering, which is very common during traffic congestion or car accidents) and to settings in which mobility patterns vary significantly over time. For these reasons, the question of how to efficiently allocate resources (i.e.,

memory, bandwidth, and infrastructure support for content seeding) for an FC scheme in a realistic setting is still an open issue to date.

In this work, we consider a setup where infrastructure support to FC (in the form of collection of data on user mobility, and orchestration of content replication) is ubiquitous. We propose *DeepFloat*, a data-based approach for dynamic management of FC in vehicular scenarios that minimizes the overall use of bandwidth and of user storage space, as well as the amount of content seeding performed by the infrastructure over the target content lifetime. Our approach adopts a Convolutional Neural Network (CNN) architecture, typically used in image processing, in order to effectively capture the complex relations between elements of a multidimensional set of system parameters, their impact on content diffusion and persistence, and the FC success ratio. Different from existing results, our approach applies to arbitrary mobility scenarios and spatio-temporal patterns of vehicle density distributions, by proactively modulating the content replication and storage strategies over time. We use a configurable cost function to flexibly account for heterogeneity in vehicles population (in terms of resource availability) and different resource cost models, as well as for the variations of these parameters over time and space. In particular, and to the best of our knowledge, our approach is the first to take explicitly into account the cost of infrastructure support to opportunistic replication, and hence to optimally adapt the balance between opportunistic replications and direct content delivery by the infrastructure to the specific context.

The numerical assessment of our approach on a set of realistic scenarios shows that it delivers very high levels of accuracy, while substantially decreasing resource costs with respect to model-based strategies. In particular, in contexts of rapidly varying mobility patterns (in which traditional approaches fail in delivering the target performance and in ensuring content persistence), we show its ability to proactively adapt content replication and availability over time in order to minimize the amount of infrastructure support to content replication in a QoS aware manner.

The paper is structured as follows. Section II presents the system model, followed by the problem formulation in Section III. Our deep learning algorithm is illustrated in Section IV and assessed numerically in Section V. Finally, Section VI concludes the paper.

II. SYSTEM MODEL

We consider a set of wireless nodes moving on the plane according to a given road grid, modeling vehicles and/or pedestrians in an urban area, with their user equipment (UE). We assume the area is served by a cellular access network, which collects data about users mobility (*floating user/car data* [10]) for optimizing its operations, coherently with the 5G (and beyond) paradigm. We assume each UE is equipped with one or more wireless technologies for direct exchange of information with other UEs via opportunistic communications, such as WIFI Direct, Bluetooth, or D2D.

We assume the surface of the road grid to be partitioned into a set of L *road links* (henceforth simply denoted as *links*). Such partition can be arbitrary, though, as we will see later, the choice of the number of links and of the and shape of each of them is based on a tradeoff between computational complexity of our approach and accuracy in the representation of the spatio-temporal mobility patterns.

We assume that two nodes are in *contact* when they are in the range to exchange information. We assume that at each time instant, the system maintains, for each road link, a list of contacts, e.g., by having nodes periodically exchange beacons. At any time, each node knows its exact position in space (i.e., its GPS coordinates).

A. *DeepFloat* FC operation

We assume that at some point in time a content (e.g., a piece of text, a picture, a short movie) is generated either by the infrastructure (e.g., an advertisement which originates from cellular or WIFI users), or by mobile nodes themselves (for instance, a warning about a road accident).

We consider a finite time interval, the *floating period*, corresponding to the period during which the content should be made available to users in a target portion of the road grid (the *Zone of Interest* or ZOI). The typical duration of the floating period ranges from half an hour up to a whole day. We assume the floating period is partitioned into T intervals, each of duration d_t , $t = 1, \dots, T$. At the beginning of the floating period, we assume that the infrastructure possesses some aggregate information about nodes mobility. This assumption is realistic as pedestrian and vehicular mobility patterns in urban scenarios exhibit predictable (and often periodic) behaviors over time [11].

A FC scheme is identified, for every road link $l = 1, \dots, L$ and time interval $t = 1, \dots, T$, by the values of *content infectivity* $a_{l,t}$, of *recovery rate* $b_{l,t}$, and of *seeding ratio* $s_{l,t}$ (with $a_{l,t}, b_{l,t}, s_{l,t} \in [0, 1]$).

At the beginning of each time interval t , the system makes sure that in each link l the percentage of nodes possessing the given content at that time (henceforth denoted as *content availability* at that time) is exactly equal to $s_{l,t}$. At the beginning of each interval t , if in each link l the content availability is less than $s_{l,t}$, the system transfers the content from the infrastructure to a number of users sufficient to achieve the target value of availability. If the initial availability is larger than the seeding ratio for that interval, the system triggers an appropriate number of users to drop the content.

In the FC scheme, at the beginning of the floating period, parameters $a_{l,t}, b_{l,t}$ are made available to each user (e.g., broadcast to all users in the area through the cellular infrastructure). In each time interval t , when two nodes come in contact, if the content is present at only one of the two nodes, the node with content transfers the content to the other node with probability $a_{l,t}$, where l is the link where the sender node resides. Such transfer is subject to all limitations of the communication capacity between the two nodes, which is influenced by propagation effects such as fading, interference,

among others. When a content is successfully transferred, the receiver (residing on link l^0) keeps it with probability $b_{l',t}$, and discards it otherwise. Moreover, for all links l , whenever a node enters link l with content, it keeps it with probability $b_{l,t}$ and drops it otherwise.

In this paper, we consider the ideal case in which nodes do not replicate content when it is not needed (i.e., when both nodes in contact already possess the content). We also assume that content exchanges are always unicast (one-to-one). However, this FC scheme can be easily extended to include the effects of multicasting and broadcasting.

The resulting matrix $\mathbf{A} = \{a_{l,t}, b_{l,t}, s_{l,t}\}$ of dimensions $L \times T$ completely describes a FC scheme. Each entry in \mathbf{A} is a 3-tuple identifying the content seeding, replication and caching strategies over all links during the whole floating period.

In each interval, if enough content replications take place after the initial seeding, the content persists over time in a portion of the road grid even when the nodes which received the initial seeding have moved out of the road grid, or discarded the content. We say in this case that the content *floats*, i.e., it persists probabilistically in the area. This usually happens for a duration which is determined by the mobility patterns, and the choice of the FC parameters \mathbf{A} , among others.

As a consequence, the primary performance metric for FC is the mean content *availability*, i.e., the mean fraction of users with content over a given time interval. Indeed, as mentioned, the goal of an FC scheme is to make the content available in a subset \mathcal{L}^0 of links in the Zone of Interest (ZOI) of the content, with a given mean availability, which we henceforth name as *success ratio* and denote with α_t . More specifically, an FC scheme aims at ensuring that, in every interval t , the condition

$$\alpha_t = \frac{\sum_{l \in \mathcal{L}^0} n_{l,t}^c}{\sum_{l \in \mathcal{L}^0} n_{l,t}} \geq \alpha_0 \quad (1)$$

is satisfied, where $n_{l,t}$ ($n_{l,t}^c$) is the mean number of users (resp. mean number of users with content) in the l -th link at interval t , and α_0 is the target minimum value of success ratio. The value of α_0 , the choice of size, shape, and location of the ZOI depend entirely on application requirements.

III. FORMULATION OF THE OPTIMIZATION PROBLEM

A cost function models the impact of an FC scheme on the number of employed resources. For each link and time interval, such function is given by the sum of three components. The first component accounts for the utilization of storage resources. For each link and time interval, it is measured by the product of the mean total number of users with content $n_{l,t}^c$ and the content size in bits, D .

The second cost component accounts for the mean amount of UE communication resources used to exchange content and it is proportional to the mean total number of UEs transmitting the content at a given time instant. Specifically, let \mathcal{U} be the

set of communication technologies available (e.g., Bluetooth, WiFi direct, D2D, LiFi), such component is given by

$$D \sum_{l,t} \sum_{u \in \mathcal{U}} \theta_{l,t,u} \gamma_{l,t,u}$$

where $\gamma_{l,t,u}$ is the mean total number of UEs transmitting the content at time interval t and link l with the u -th technology. The coefficient $\theta_{l,t,u}$ can be used to modulate the cost of opportunistic content exchanges across technologies, links and time intervals, in order to take into account the availability of resources in that technology (e.g., due to utilization, to interference levels), and of the way it varies over time. In general, $\gamma_{l,t,u}$ depends on content size, available bandwidth, and the distance between transmitter and receiver.

The third cost component takes into account the number of content transfers, implemented directly through the infrastructure (e.g., through the cellular network), for seeding the content in those links in which the availability at the beginning of a given time interval is inferior to the target seeding ratio. Hence, it is given by

$$D \sum_{l,t} [s_{l,t} - v_{l,t}]^+$$

(where $\forall x, [x]^+$ stands for $\max(x, 0)$), and it is based on the assumption that content suppression “comes for free”. $v_{l,t}$ is the availability at the beginning of interval t , *before* content seeding. It is given by

$$v_{l,t} = \begin{cases} 0 & t = 1 \\ \frac{n_{l,t-1}^c}{n_{l,t-1}} & t > 1 \end{cases} \quad (2)$$

An optimal FC scheme \mathbf{A} is hence a solution to the following problem:

Problem 1 (FC resource optimization):

$$\min_{\mathbf{A}} \sum_{l,t} \frac{d_t D (n_{l,t}^c + \beta \sum_{u \in \mathcal{U}} \theta_{l,t,u} \gamma_{l,t,u})}{\sum_t d_t} + \delta D [s_{l,t} - v_{l,t}]^+ \quad (3)$$

$$\forall t, \quad \alpha_t \geq \alpha_0 \quad (4)$$

$$\forall t, l \quad 0 \leq a_{l,t} \leq 1, \quad 0 \leq b_{l,t} \leq 1, \quad 0 \leq s_{l,t} \leq 1 \quad (5)$$

The overall cost function is given by the sum of the three components, of which two (the ones related to storage and opportunistic content exchanges) are weighted by the ratio between the interval duration and the duration of the whole floating period, $\sum_{t=1}^T d_t$. Coefficients $\beta, \delta \geq 0$ modulate the relative weight of the three cost components (memory, bandwidth, and seeding) on the overall cost of an FC scheme. These coefficients, together with $\theta_{l,t,u}$, are the instruments by which network operators can orchestrate the Floating Content service. Among all the possible FC schemes \mathbf{A} , a special role is played by the one in which $\forall l, t, a_{l,t} = b_{l,t} = s_{l,t} = 1$. With such choice, the content is replicated at every opportunity over the whole road grid, and it is never dropped. This scheme, which we call *all-on*, allocates all user resources in the system

to the FC communication scheme and guarantees that at the beginning of each interval, each user possesses the content. This implies that for each time interval, the all-on scheme achieves the highest possible value of success ratio in the considered scenario. Therefore, if the all-on scheme is not a feasible solution of Problem 1, the problem is infeasible. When this is the case, Problem 1 has to be reformulated by providing more resources to FC, e.g., by considering a larger road grid, by including a larger population of users, by changing α_0 or communication technologies.

In general, Problem 1 cannot be solved efficiently. Indeed, in general $\forall l, t, n_{l,t}^c$ and $\gamma_{l,t,u}$ depend on \mathbf{A} as well as on a large set of parameters, in ways which are hard to accurately capture analytically without strong and unrealistic assumptions, such as stationarity of mobility patterns and uniformity of user distributions. In the next section, we present our approach to this intractable problem, based on Deep Learning.

IV. A DEEP LEARNING ALGORITHM FOR EFFICIENT FC DIMENSIONING

In this section, we illustrate our DeepFloat approach to finding an efficient solution of Problem 1. It is based on Convolutional Neural Networks (CNN), a specialized type of neural network which has proven particularly effective in modeling data with grid-like topology [12]. The key idea of our approach is to exploit this CNNs property in order to accurately and efficiently model the correlation between the spatial features of the road grid, and the way in which the content spreads among links and persists over time. Our approach is divided into three phases:

Offline Set Up. The cellular infrastructure collects and records UE mobility traces over time across the whole road grid, on a regular basis. The training set is generated, by associating the communication features to the measured mobility features. Finally, the CNN is trained.

Bootstrap. It starts when an application (which may or may not reside within a UE) requests to the system, via the cellular infrastructure, the activation of an FC scheme, with a given ZOI, target success ratio, and floating period. The system, given the forecasted resource availability and mobility patterns, uses the trained CNN to compute in real time a strategy \mathbf{A} that achieves the target success ratio.

Deployment. The system provides to all UEs present in the considered road grid at the beginning of the floating period (as well as to all those UEs which enter the road grid during the floating period) the coefficients $a_{l,t}$ and $b_{l,t}$ which identify the replication and caching strategy derived by the CNN. At the beginning of each time interval, in each link, the content is seeded according to $s_{l,t}$. If necessary (i.e., if, during the floating period, mobility patterns in the road grid deviate significantly from the forecasted ones), new forecasts are elaborated, and a new strategy \mathbf{A} is adopted for the rest of the floating period.

In what follows, we describe in detail the three phases, and the algorithms involved.

A. Offline Set Up

1) *Data collection:* As we have mentioned, the system collects, on a regular basis, data about UEs mobility in the grid. Specifically, we assume that the system partition time into intervals. For each time interval, the system records the trajectories of each UE in the grid.

Starting from these trajectories, for each interval i , and every link l , the system computes a set of aggregate metrics relative to node mobility and to wireless communications. In what follows, these metrics are the average node speed, the average number of nodes, and average contact duration. In addition, it computes the mean number of nodes that, in a given time instant, are in contact (i.e., able to exchange beacons) with a node. These parameters have been chosen as they are typically used as input in the main existing analytical models of FC [4], [5]. Of course, however, different choices are possible. In general, the choice of the set of parameters, as well as the aggregation level in space (i.e., size and shape of links) and time (i.e., duration of an interval d) affects the degree of accuracy with which our model accounts for the spatio-temporal features of the system, and specifically, for the mobility patterns. The parameters values, for each interval i and link, are stored in a *mobility feature array* \mathbf{m}_i .

2) *Label generation:* In the next step, called *label generation*, a randomization procedure is applied. Specifically,

for each \mathbf{m}_i , a set of K random FC schemes \mathbf{A}_k , $k = 1, \dots, K$ are generated, each with its seeding strategy.

For each i and each couple $(\mathbf{m}_i, \mathbf{A}_k)$, a simulation is performed based on the random strategy \mathbf{A}_k and the user trajectories during interval i . For each communication technology, these simulations assume a given model for the channel capacity between nodes over time. The parameters measured, for each link, are the mean number of nodes with content at a given time instant $n_{l,i}^c$, and the mean number of nodes that are transmitting at a given time instant for each communication technology, $\gamma_{l,i,u}$. Both these quantities are averaged over the duration of the interval. These parameters constitute the *communication feature vector*, \mathbf{c}_i . Given a choice of ZOI, these parameters are the basis for the computation of the success ratio, as well as for the estimation of the resource utilization and of the associated cost. However, note that the knowledge of the ZOI or of the target success ratio is not required to produce the training set. Hence this phase can be performed entirely offline.

For each k and i , with $\mathbf{P}_i = (\mathbf{m}_i, \mathbf{c}_i)$ we denote the *Link Features Vector* associated with \mathbf{A}_k (Table I). Finally, each vector \mathbf{P}_i is normalized, in order to avoid numerical issues in the subsequent phases of the process. The output of the offline phase is thus a set of pairs $(\mathbf{P}_i, \mathbf{A}_k)$, which we denote with \mathcal{S} . The set \mathcal{S} is therefore enriched over time with new elements derived by simulations. In addition to those elements, the system includes in \mathcal{S} also those elements derived by directly measuring FC performance (specifically, those in the communication feature vector) during the operation of the FC schemes. Note that, while the presence of such measured

TABLE I: The set of link features for time interval i and link l .

Name	Description
$n_{l,i}^c$	average number of nodes with content
$n_{l,i}$	average number of nodes
$\lambda_{l,i}$	average number of nodes in contact
$\tau_{l,i}$	average contact duration [s]
$\nu_{l,i}$	average speed [m/s]
$\gamma_{l,i,u}$	average number of nodes transmitting in the u th technology

elements helps in achieving a high level of accuracy in real scenarios, the contribution to of those elements derived through simulations plays a key role in enabling the system to appropriately configure an FC scheme in those scenarios which occur with a relatively low frequency (e.g. road accidents, sport events, disasters).

B. Bootstrap and Deployment

The bootstrap phase starts when a request for FC service is made. A request is characterized by an indication of the region of the road grid which constitutes the ZOI, by the target value of success ratio α_0 , and by the floating period.

In what follows we assume the floating period to be composed by T intervals, and let \mathbf{m}_t be the mobility feature array for the t -th interval, $t = 1, \dots, T$. $\forall t$; we assume the arrays \mathbf{m}_t to be perfectly known at the time of the service request, possibly by forecasts based on the mobility traces which the system collects on an ongoing basis (we will later describe how our approach accounts for forecast errors).¹ Given $\mathbf{M} = \mathbf{m}_1, \dots, \mathbf{m}_T$ the forecasted mobility features for the floating period, the definition of the ZOI (i.e. the set \mathcal{L}^b), and the target success ratio, the CNN computes the replication, caching, and seeding strategies $\mathbf{A} = \mathbf{A}_1, \dots, \mathbf{A}_T$ for the whole floating period, which achieve the target success ratio while trying to minimize the resource cost as defined in (3). For these strategies, the content infectivity, as well as the recovery rate for each link and time interval within the floating period are communicated to all nodes in the scenario. In those cases in which, during the operation of an FC scheme, better forecasts of mobility become available, the system computes a new strategy \mathbf{A} for the remaining portion of the floating period, based on such forecasts, and it injects the new values of content infectivity and recovery rates to all the nodes.

C. CNN Model Architecture

In this section we describe the architecture of the CNN adopted in our approach.

In the FC dimensioning problem, the information about proximity or relative position between links is not part of the link features. In general, the correlations between features of different road links are not due only to proximity. Rather, they are also the result of wireless propagation effects and, most importantly, of spatio-temporal patterns in node mobility (i.e., typical patterns of vehicular traffic).

¹The mechanism by which these arrays are forecasted is out of the scope of the present paper

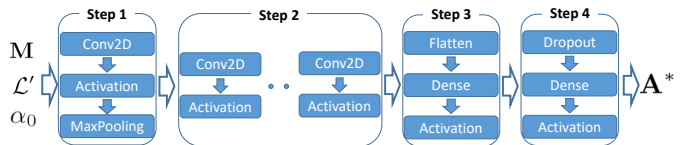


Fig. 1: Outline of the architecture of our Convolutional Neural Network. It takes as input the mobility features \mathbf{M} , as well the set of links composing the ZOI, \mathcal{L}^b , and the target success ratio α_0 . Its output are the replication, caching, and seeding strategies \mathbf{A}^* .

The Convolutional Neural Network (CNN) architecture enables capturing both intra-link and inter-link relations between features. The features extracted by our CNN are associated with the correlation between road links. As a result, the characteristics extracted from each layer of the CNN do not consist only in local correlations, but also in long-spatio-temporal relations between links, which have a strong impact on FC performance.

The detailed structure of the CNN architecture consists of four steps (Fig. 1). The goal of step 1 is to learn features corresponding to basic patterns in the input (e.g., the strongest local correlations, such as the spatio-temporal correlations between adjacent road links and between the features of the same road link.) [12]. Step 1 consists in a convolution layer, which filters the input data (layer *Conv2D* in Fig. 1). The size of the convolution kernel determines the extent of the locality of the correlations captured. The output is fed into an *activation layer*, followed by a discretization process (*max pooling* layer). The purpose of these two layers is to filter out information which will not be relevant for subsequent parameter optimization.

Step 2 consists typically in a number of blocks which repeat the same operations as step 1 without the maxpooling layer. The number of these layers directly determines the depth of the CNN, and therefore the level of complexity of the correlations it is able to capture. Hence their number depends on the characteristics of the modeled system, but also on a tradeoff between computational complexity and accuracy of the output. The choice of kernel size in the Conv2D layers should also be done according to such tradeoff. Indeed, a small kernel forces the use of several convolution steps in order to capture long-range correlations. A large kernel instead decreases the amount of Conv2D layers required in step 2, but it also prevents the CNN from accurately modeling complex correlations. The purpose of step 3 is to reshape the output of the previous step, in order to facilitate the subsequent computations. Its output is a set of candidate strategies for orchestrating our FC system. Finally, step 4 performs an optimization over these candidate strategies, by selecting out iteratively those who do not satisfy the performance constraint on success ratio, and by giving as output the one which minimizes the cost function in (3).

A crucial aspect of the performance of our approach is the computational load required by the three phases which compose it. Given the potentially large amount of data to be collected and pre-processed, the offline set up is the most computationally intensive phase, being directly related to the

size of the set \mathcal{S} , as well as to the number of links and features considered. However, given that all the elaborations in the offline setup phase are executed offline, they do not impact the delay with which a request for a floating content is served.

Conversely, the computations required by the bootstrap phase are performed in real time at the moment in which a request is made. Therefore, those effects heavily affect the overall FC performance, particularly for those applications for which a quick and effective deployment of the FC scheme is often necessary such as car accident warning or medical emergency notification. In order to enable a fast deployment in these scenarios, several ways exist to decrease the computational load at the bootstrap time within our approach. A possibility, as discussed, is to adopt a low number of blocks at step 2 in the CNN. Another, it is to solve Problem 1 only for the first of the T intervals which compose the floating period, thus allowing the system a longer time to compute the optimal strategy for the rest of the floating period. Finally, another way is to decrease the dimensionality of the problem, by setting $\forall l, t, s_{l,t} = b_{l,t}$. This corresponds to imposing that the number of users with content at the beginning of each interval to coincide with the probability to keep the content once received, which in our FC system is clearly strongly correlated with (though typically inferior to) the availability in the given interval and link.

V. NUMERICAL EVALUATION

In this section, we assess the performance of our DeepFloat algorithm numerically, in terms of model accuracy and resource efficiency, and we characterize the spatio-temporal strategies emerging from it.

A. System setup

We assumed nodes use a single wireless communication technology, with a channel model typical of urban scenarios, a SINR value equal to 5 dB (which models setups with high interference, common in crowded city centers, e.g. at the 2.4 GHz frequency), content size $L = 4$ MB (to emulate the exchange of multimedia content such as pictures and short videos), bandwidth $B = 1$ MHz (as in Bluetooth) and the channel capacity resulting from Shannon's formula. Unless otherwise specified, the FC parameters and those of the CNN have been chosen conservatively in order to fit a worst case scenario, in which applications require a fast bootstrap phase, a relatively short content floating period ($1h$), and a high level of target success ratio (0.9). Both β and δ in the cost function (3) are set to 1 (to have replication, caching, and seeding equally contributing). As we show in this section, a CNN architecture with a single block at step 2 and a Conv2D kernel of size 3-by-3, together with the seeding approximation described in Section IV-C have proven sufficient to achieve a good level of accuracy while minimizing computational load. In order to avoid over-fitting, a standard 10-fold cross-validation is performed.

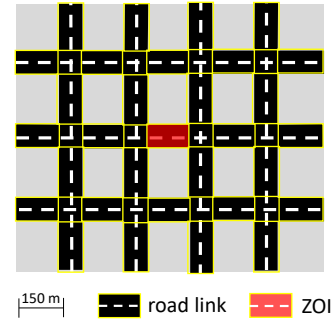


Fig. 2: Manhattan road grid composed of 5-by-4 square blocks of side 150 m, for a total of 31 road links and 12 road intersections.

B. Manhattan scenario

In the first set of experiments, we evaluated the performance of our proposed approach in a scenario with synthetic mobility, in order to perform, in a controlled scenario, a first-order characterization of the strategies emerging from the DeepFloat approach, and of their effectiveness and efficiency.

We considered the road grid in Fig. 2. Nodes enter and exit the grid from road links at the border, with an arrival rate equal to 3 nodes/s per road link, equal for all road links. At every crossroad, a new direction is chosen at random between straight, right and left. The floating period is composed by a single interval of 1h duration.

The training set was built as follows. The road link features were measured over $1h$, using a sampling interval of 1s. In order to collect communication features, we considered 10^3 different random strategies. The resulting simple randomization, in each scenario, contained about $4 \cdot 10^6$ pairs (\mathbf{P}, \mathbf{A}) . In this paper, to study model accuracy despite prediction quality, we assume that mobility is predicted perfectly.

1) *Model Accuracy*: In order to evaluate the accuracy of our algorithm, Fig. 3 shows the values of F-score [13] versus the training set size, for three different combinations of transmission radius and speed ($r = 100$ m and speed $\nu = 60$ km/h; $r = 100$ m and ν uniformly distributed in $[0, 60]$ km/h; $r = 500$ m and $\nu = 60$ km/h). In each scenario, we also computed the performance of other algorithms for multi-labeled classification problems, i.e., K-Nearest Neighbor (KNN), Decision Tree (DT), and Random Forest (RF). Note that for each algorithm, all scenarios are tested using over $1.5 \cdot 10^5$ registers of the test set, obtaining a high sample population for the confidence interval.

Results in Fig. 3 show that DeepFloat substantially outperforms the other algorithms in terms of accuracy. In particular, our approach achieves a high accuracy even with small training sets. This confirms that for the problem of efficient dimensioning of an FC scheme, the specific ability of CNNs to capture the inter-link correlations is key for satisfactory performance. This is also suggested by the fact that, by increasing the transmission radius (and hence the amount of inter-link content exchanges), the relative accuracy of our approach improves.

A key aspect of any learning approach to FC dimensioning is that even approaches with high accuracy may produce

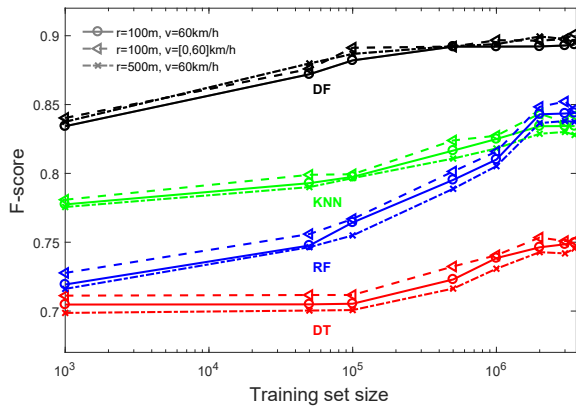


Fig. 3: F-score versus size of the training sample, for the DeepFloat approach (DF), as well as for K-Nearest Neighbor (KNN), Decision Tree (DT), and Random Forest (RF), for the three scenarios considered. All curves are with a 98% confidence interval of 7%

TABLE II: Rejection probability (i.e., probability of not achieving the target success ratio) of the four approaches considered. Values are with a 98% confidence interval within 6% of interval size. Training set size: $1.5 \cdot 10^5$.

Transmission radius [m]	100	100	500
Speed [km/h]	60	[0, 60]	60
DF	0.029	0.031	0.032
KNN	0.274	0.287	0.284
RF	0.324	0.320	0.333
DT	0.347	0.345	0.349

configurations that are unfeasible, i.e., which do not achieve the target performance. Table II shows, for all considered scenarios and algorithms, the probability that the output of the learning processes does not satisfy constraint (4). For our approach, the rejection probability is around 3%, an order of magnitude lower than for the other considered approaches. Indeed, CNNs tend to decrease the *false positive* predictions rather than the *false negative* ones. This is due to the fact that, for any input, in the search for the strategy which minimizes resource cost, our approach always considers the all-on configuration as a fallback option.

2) *Resource Optimization*: A crucial performance parameter of our CNN approach is the percentage of resources saved with respect to the all-on configuration. Such a configuration is considered as a reference, as by hypothesis it is the only one that is always feasible. Fig. 4 shows the percentage of resources saved with respect to the trivial case of the all-on configuration. They have been computed assuming that those configurations that do not achieve the target success ratio have the same cost of the all-on configuration. In the figure, we present both the ideal case where no predicted configuration has been rejected, and the case which takes into account the rejected outputs. In the ideal case, by using the Decision Tree technique we save up to 39% of the resources with respect to the all-on configuration. However, not all configurations resulting from DT satisfy the success ratio constraint. These results suggest that our CNN architecture is able to shape the content replication and storage strategies much more efficiently than classical, non-deep ML techniques.

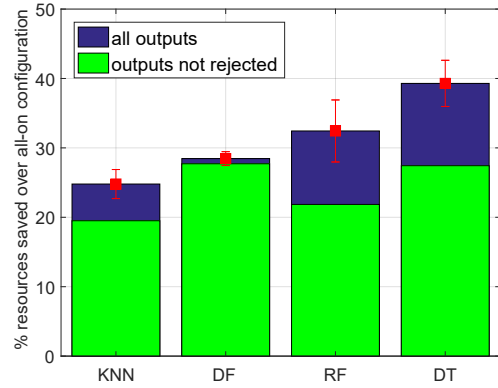


Fig. 4: Percentage of resources saved with respect to the all-on strategy, for the four approaches considered. $r = 100m$ and $v = 60km/h$. Values are with the confidence interval of 98% with interval size of 3%.

Indeed, differently than these techniques, our CNN is able to take advantage of the very high number of parameters used for training, achieving high accuracy without requiring a large training set or any geographical information (such as a road map).

C. Luxembourg City scenario

In order to perform a more realistic assessment of the performance of our approach, we considered a second scenario, shown in Fig. 5. It consists of two districts (denoted as Residential and City center). In both districts, the street grid and the measurement-based mobility traces for the rush traffic hour (i.e., between 7 AM and 8 AM) were derived from [14]. These areas were selected because of their difference in vehicles density distribution. In the city center, during the rush hour, the vehicle density distribution is high and relatively uniform, while in the residential district it is lower and more clustered. In both scenarios, we considered as ZOI the closest link to the center of the district. In both districts, we collected data from 169 road links, using a sampling rate of 1s to accurately capture mobility dynamics. The transmission radius is taken to be 100m (such as in Bluetooth Low Energy). We assumed a floating period composed by a single interval of 1 h, (adequate for a traffic warning e.g., about a temporarily restricted area). By choosing a single interval, we focus on the ability of the considered approaches to capture spatial correlations in the input data.

In Table III, we list the test accuracy values obtained by using $1.5 \cdot 10^5$ registers for testing, and 10^6 for training. While non-deep learning techniques have a worse accuracy in the Luxembourg scenario than in the Manhattan one, the contrary holds for DeepFloat, which is able to account for spatial inhomogeneities in the mobility features.

The main existing analytical result which addresses the issue of resource-optimal FC dimensioning in a road grid was presented in [4]. It assumes that content is replicated and stored within a circular area (called anchor zone - AZ) within which content infectivity and recovery rate are both set to 1.

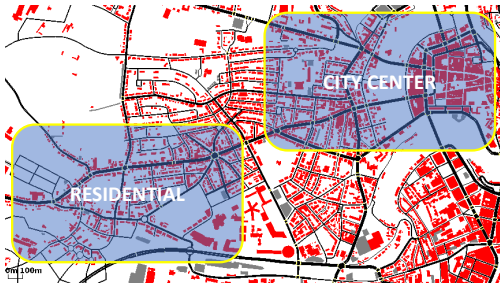


Fig. 5: Luxembourg City map, with the borders of the City center and Residential areas.

TABLE III: F-score for the Manhattan and Luxembourg scenarios, with a training set size of 10^6 , and test set size of $1.5 \cdot 10^3$.

		DF	KNN	RF	DT
Manhattan	$r = 100m$ $v = 60km/h$	0.892	0.824	0.810	0.738
	$r = 100m$ $v = [0, 60]km/h$	0.893	0.834	0.816	0.740
	$r = 500m$ $v = 60km/h$	0.894	0.819	0.802	0.736
	city center	0.897	0.802	0.800	0.726
Lux.	residential	0.896	0.798	0.801	0.722

For the two districts of Luxembourg City, we have evaluated the resource efficiency of our DeepFloat approach, as well as of the KNN, Decision Tree, and Random Forest approaches, in terms of percentage of resources saved with respect to the approach from [4]. As in the Manhattan scenario, we have assumed that the cost of rejected outputs is the same as the one of the all-on configuration. As we can see, all ML approaches outperform the analytical result. This is most likely due to the fact that the analytical approach is based on an assumption of uniformity of the main mobility features within the AZ. Indeed, the gains over the analytical result are larger in the less-uniformly distributed residential scenario than in the city center.

Table IV provides the output rejection probability for the Luxembourg scenarios. Similarly to the Manhattan scenario, the lowest values are provided by the DeepFloat approach in the city center (1.8%).

Bottom line, these results suggest that in realistic, hereogeneous vehicular scenarios our DeepFloat approach significantly outperforms the best available analytical approach, as well as some of the main non-deep learning approaches, both in terms of efficiency and accuracy.

D. Temporal dynamics of the DeepFloat strategies

In a last set of experiments in the Luxembourg scenario, we have aimed at a first order characterization of the temporal dynamics of the strategies emerging from our approach. To this end, we have considered the same 1 h floating period to be composed by two intervals of equal duration. The ZOI definition, as well as the target success ratio are the same as in the previous experiments. About 400 simulations experiments have been run, to achieve an uncertainty of 0.05% within

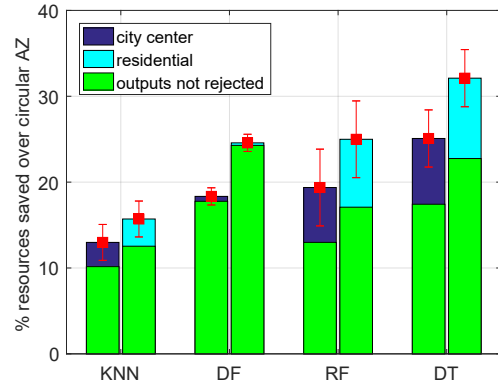


Fig. 6: % of resource saved with respect to the Circular Anchor Zone approach [4], for our DeepFloat approach (DF), as well as for the K-Nearest Neighbor (KNN), Decision Tree (DT), and Random Forest (RF) approaches, in the rush hour time interval. Confidence interval of 98% with interval size of 3%.

TABLE IV: Rejection probability of the considered ML approaches. Values are with a 98% confidence interval within 6% of interval size. Luxembourg scenario.

Method	City Center	Residential
DF	0.018	0.021
KNN	0.224	0.229
RF	0.307	0.314
DT	0.332	0.341

a confidence interval of 95%. Figure 7 shows the number of vehicles in the district as a function of time during the two intervals. In the second interval, the average number of vehicles is about 50% higher than in the first interval. In an unconstrained setting, high vehicular density calls for high resource allocation for both replication and caching.

Fig. 8 shows the box-plots, with interquartile range (IQR) and population median (in red), of the success ratio obtained by simulating the strategies from the DeepFloat approach. Outliers exit the $Q_x \pm 1.5 IQR$, with $x \in \{1, 3\}$ quartile Q . As shown, our strategies allow the system to achieve in both intervals the minimum value of success ratio (0.9).

As we have observed, strategies emerging from our DeepFloat approach try to minimize, for each link, the difference between the amount of seeding required at the beginning of each interval, and the mean availability at the previous interval. In this way, it produces strategies which try to modulate the distribution of content in an interval in a way which takes also into account the seeding requirements at the following interval. With the given choice of coefficients ($\beta, \delta = 1$), in the whole set of simulations no seeding support has been necessary at the the beginning of the second interval, in any link. This suggests the effectiveness of our approach in accurately controlling content availability in space and time as a function of resource cost, and in particular, in decreasing infrastructure support whenever its cost becomes higher than the cost of using hosts resources.

Another evidence of the dynamic adaptation of the temporal strategy to traffic conditions is shown in Figure 9 and 10.

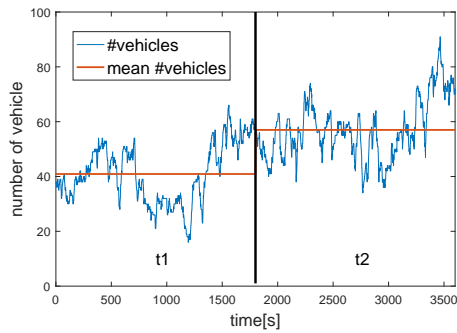


Fig. 7: Vehicle density over time in the Luxembourg city center scenario, for the first time interval $t_1 = (7 \text{ AM} - 7:30 \text{ AM})$, and for the second, $t_2 = (7:30 \text{ AM} - 8 \text{ AM})$.

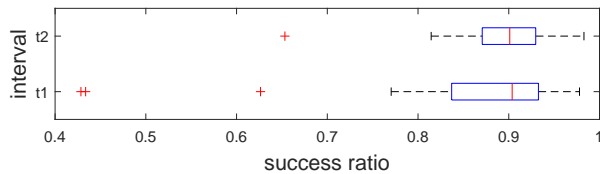


Fig. 8: Distribution of the measured success ratio derived with the strategies from the DeepFloat approach, in time interval $t_1 = (7 \text{ AM} - 7:30 \text{ AM})$ and $t_2 = (7:30 \text{ AM} - 8 \text{ AM})$, for the Luxembourg city center scenario.

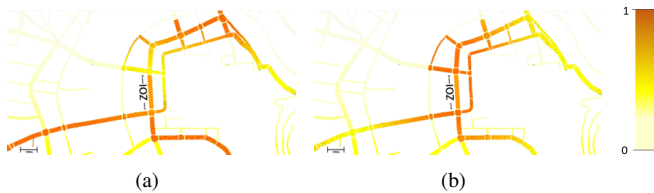


Fig. 9: Luxembourg city center replication strategy at $t_1 = (7 \text{ AM} - 7:30 \text{ AM})$ (a) and $t_2 = (7:30 \text{ AM} - 8 \text{ AM})$ (b).

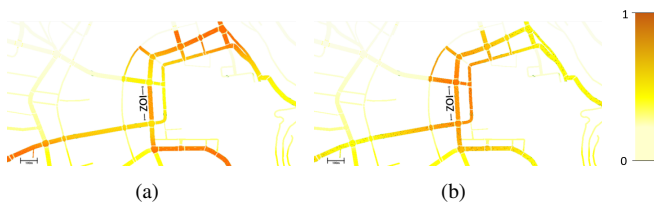


Fig. 10: Luxembourg city center storage strategy $t_1 = (7 \text{ AM} - 7:30 \text{ AM})$ (a) and $t_2 = (7:30 \text{ AM} - 8 \text{ AM})$ (b).

To counter the increase in vehicle density while meeting the performance target at t_2 , the system effectively adapts both replication and caching areas. Figures 9(b) and 10(b) shown how the system activates only those resources near the ZOI that are necessary to achieve the performance target. On the other hand, the system lowers replication and caching probabilities where possible, to avoid unnecessary resource usage (see the north-west areas in Figures 9 and 10).

E. Time considerations

In the Luxembourg scenario, characterized by 167 links, and on a I7 desktop PC with 16 GB of RAM, the first two

phases of our approach (training set buildup and CNN training) together took 3s for a training set of 10^3 batches, and about 3 min for 10^6 batches. Hence, at least in the considered scenario (i.e., a whole city center), and with the given choices of links and parameters, the computational load of the offline phase does not require a large number of resources. As for the bootstrap phase, in all our experiments, the computation of the FC strategy by the CNN always took less than one second, suggesting that, despite the large road grid and the large size of the training set considered, our approach is fit for real-time operation while keeping an excellent level of accuracy.

VI. CONCLUSIONS

In this work, we have outlined a Deep Learning approach for efficient FC dimensioning, which exploits a Convolutional Neural Network to modulate over time the parameters governing a FC service. We have shown on realistic, measurement-based scenarios that our approach efficiently shapes the communication area and optimizes replication, caching, and seeding strategies, while achieving the desired QoS targets over time. Among the possible extensions to our approach, in the followup we intend to consider those to scenarios in which mobility patterns are influenced by the spreading of content (e.g., traffic jams notification).

REFERENCES

- [1] 5GPP, "White paper: 5G empowering vertical industries," Tech. Rep., February 2016.
- [2] D. Jiang and L. Delgrossi, "IEEE 802.11p: Towards an international standard for wireless access in vehicular environments," in *IEEE VTC Spring*, May 2008.
- [3] E. Hyttia, J. Virtamo, P. Lassila, J. Kangasharju, and J. Ott, "When does content float? Characterizing availability of anchored information in opportunistic content sharing," *IEEE INFOCOM*, April 2011.
- [4] G. Manzo, R. Soua, A. Di Maio, T. Engel, M. R. Palattella, and G. Rizzo, "Coordination mechanisms for floating content in realistic vehicular scenarios," in *IEEE MobiWorld*, April 2017.
- [5] G. Manzo, M. A. Marsan, and G. Rizzo, "Performance modeling of vehicular floating content in urban settings," in *ITC 29*, September 2017.
- [6] J. M. Duarte, E. Kalogeiton, R. Soua, G. Manzo, M. R. Palattella, A. D. Maio, T. Braun, T. Engel, L. A. Villas, and G. A. Rizzo, "A multi-pronged approach to adaptive and context aware content dissemination in VANETs," *Mobile Networks and Applications*, January 2017.
- [7] J. Kangasharju, J. Ott, and O. Karkulahti, "Floating content: Information availability in urban environments," in *IEEE PERCOM*, March 2010.
- [8] S. Ali, G. Rizzo, V. Mancuso, and M. A. Marsan, "Persistence and availability of floating content in a campus environment," *IEEE INFOCOM*, March 2015.
- [9] M. S. Desta, E. Hyttia, J. Ott, and J. Kangasharju, "Characterizing content sharing properties for mobile users in open city squares," in *10th WONS*, March 2013.
- [10] A. Dhamaniya and S. Chandra, "Speed prediction models for urban arterials under mixed traffic conditions," *Procedia - Social and Behavioral Sciences*, vol. 104, January 2013.
- [11] L. Ghouti, T. R. Sheltami, and K. S. Alutaibi, "Mobility prediction in mobile ad hoc networks using extreme learning machines," *Procedia Computer Science*, vol. 19, March 2013.
- [12] I. Goodfellow, Y. Bengio, and A. Courville, *Deep learning*. MIT press Cambridge, March 2016.
- [13] Y. Sasaki, "The truth of the F-measure," *Teach Tutor Mater*, January 2007.
- [14] L. Codeca, R. Frank, and T. Engel, "Luxembourg SUMO Traffic (LuST) Scenario: 24 hours of mobility for vehicular networking research," in *VNC*, December 2015.